

Effects of drive imbalance on the particle emission from a Bose-Einstein condensate in a one-dimensional lattice

Long-Quan Lai(赖龙泉) and Zhao Li(李照)

Citation: Chin. Phys. B, 2024, 33 (**3**): 030308. DOI: 10.1088/1674-1056/ad1172
Journal homepage: http://cpb.iphy.ac.cn; http://iopscience.iop.org/cpb

What follows is a list of articles you may be interested in

Enhanced measurement precision with continuous interrogation during dynamical decoupling

Jun Zhang(张军), Peng Du(杜鹏), Lei Jing(敬雷), Peng Xu(徐鹏), Li You(尤力), and Wenxian Zhang(张文献)
Chin. Phys. B, 2024, 33 (**3**): 030301. DOI: 10.1088/1674-1056/ad1985

Dynamical nonlinear excitations induced by interaction quench in a two-dimensional box-trapped Bose-Einstein condensate

Zhen-Xia Niu(牛真霞) and Chao Gao(高超)
Chin. Phys. B, 2024, 33 (**2**): 020314. DOI: 10.1088/1674-1056/ad1179

Special breathing structures induced by bright solitons collision in a binary dipolar Bose-Einstein condensates

Gen Zhang(张根), Li-Zheng Lv(吕李政), Peng Gao(高鹏), and Zhan-Ying Yang(杨战营)
Chin. Phys. B, 2023, 32 (**11**): 110303. DOI: 10.1088/1674-1056/acf283

Mode dynamics of Bose-Einstein condensates in a single-well potential

Yaojun Ying(应耀俊), Lizhen Sun(孙李真), and Haibin Li(李海彬)
Chin. Phys. B, 2023, 32 (**10**): 100310. DOI: 10.1088/1674-1056/acdedb

Nonlinear modes coupling of trapped spin-orbit coupled spin-1 Bose-Einstein condensates

Jie Wang(王杰), Jun-Cheng Liang(梁俊成), Zi-Fa Yu(鱼自发), An-Qing Zhang(张安庆),Ai-Xia Zhang(张爱霞), and Ju-Kui Xue(薛具奎)
Chin. Phys. B, 2023, 32 (**9**): 090305. DOI: 10.1088/1674-1056/accd53

Effects of drive imbalance on the particle emission from a Bose–Einstein condensate in a one-dimensional lattice

Long-Quan Lai(赖龙泉)[1,†] and Zhao Li(李照)[2,‡]

[1] *School of Science, Nanjing University of Posts and Telecommunications, Nanjing* 210023, *China*
[2] *School of Electronic Engineering, Chengdu Technological University, Chengdu* 611730, *China*

(Received 24 August 2023; revised manuscript received 3 November 2023; accepted manuscript online 1 December 2023)

Time-periodic driving has been an effective tool in the field of nonequilibrium quantum dynamics, which enables precise control of the particle interactions. We investigate the collective emission of particles from a Bose–Einstein condensate in a one-dimensional lattice with periodic drives that are separate in modulation amplitudes and relative phases. In addition to the enhancement of particle emission, we find that amplitude imbalances lead to energy shift and band broadening, while typical relative phases may give rise to similar gaps. These results offer insights into the specific manipulations of nonequilibrium quantum systems with tone-varying drives.

Keywords: Bose–Einstein condensate, particle emission, periodic drive

PACS: 03.75.Kk, 03.75.Nt, 05.30.Jp **DOI:** 10.1088/1674-1056/ad1172

1. Introduction

Ultracold atomic experiments have become a versatile platform to extensively investigate quantum many-body systems during the past decades. Numerous advances enable the explorations on a wide range of interdisciplinary topics, such as novel quantum states,[1–3] nonequilibrium dynamics,[4,5] and quantum simulations.[6–8] In the out-of-equilibrium many-body physics, time-periodic driving is an exciting tool for coherently manipulating the interparticle interactions,[9] which provides new insights into topological states,[10,11] synthetic gauge fields[12] and modulated lattices,[13–16] and leads to some striking phenomena, e.g., the stimulated particle jets resembling fireworks.[17]

In that visually appealing experiment, researchers periodically modulated the magnetic field near the Feshbach resonance,[18] and hence made the scattering length of the atoms in the condensate oscillate sinusoidally. Pair of excited atoms shared half of the drive energy, and escaped from the trap in antipodal directions, resulting in significant particle jets. Such amplification offers stimulating applications in quantum metrology and simulation of highly nonequilibrium systems. Subsequently, a number of experimental and theoretical groups have performed a series of follow-up investigations and revealed various new aspects,[19–26] e.g., the jet substructure in nonuniform and rotating condensates[20] and correlated jets from a driven matter-wave soliton.[22] In particular, semi-infinite and infinite lattice models were introduced to mimic the behaviors of the trapped particles in a transparent way,[27,28] where the time evolution of the atoms in the horizontal plane was simulated by the hopping of particles from the condensate to the "leads" and between neighboring sites, and the spatial expansion was simply limited in one dimension.

Simultaneous manipulations were often employed to the condensates in generic studies, while it might be interesting to separately vary the drives. In some other contexts, time-periodic drivings with tone-varying frequencies were applied, such as pattern formation in a driven condensate,[21] topological Floquet engineering and pumping in optical lattices.[29–31] In a previous work, we analyzed a minimal one-dimensional lattice model where the trap contains two sites, and periodically modulated the interparticle interactions to study the parametric resonance of particle emission from a Bose–Einstein condensate.[28] We now turn to a similar system, however, with periodic drives that are separate in modulation amplitudes and relative phases, and follow the perturbative framework developed in Ref. [28] to explore the collective emission of particles. We discuss various cases with different modulation amplitudes and relative phases, where imbalanced drives may result in the distinct enhancement of the emission and the redistribution of energy bands. For clarity, we also give intuitive illustrations of the influences.

The paper is organized as follows. In Section 2, we introduce the two-site lattice model and discuss the formalism of dealing with such a system. In Section 3, we present the numerics and discussions based on perturbative analysis, and compare different cases of drives by varying the modulation amplitudes and relative phases, respectively. Finally, we summarize our results in Section 4.

[†]Corresponding author. E-mail: lqlai@njupt.edu.cn
[‡]Corresponding author. E-mail: leezhao@hnu.edu.cn

© 2024 Chinese Physical Society and IOP Publishing Ltd

2. Theoretical model

We consider the situation of a one-dimensional infinite lattice, where a local trapping potential of depth V is applied to confined the Bose–Einstein condensate, as shown in Fig. 1. Two central sites, labeled a and b, are coupled with amplitude J_{ab}, which allows the transfer of atoms from one site to the other. When the perturbations are turned on, excited particles with sufficient energy can escape from the trap and travel to infinity, by hopping onto one of the two leads with coupling strength $J_{\rm c}$ and moving between nearest-neighbor sites with amplitude $J_{\rm l}$. The Hamiltonian is thus written as

$$\begin{aligned}\hat{H} =& V(\hat{a}_0^\dagger\hat{a}_0+\hat{b}_0^\dagger\hat{b}_0)+\frac{1}{2}[U+g_a(t)]\hat{a}_0^\dagger\hat{a}_0^\dagger\hat{a}_0\hat{a}_0\\&+\frac{1}{2}[U+g_b(t)]\hat{b}_0^\dagger\hat{b}_0^\dagger\hat{b}_0\hat{b}_0-J_{ab}(\hat{a}_0^\dagger\hat{b}_0+\hat{b}_0^\dagger\hat{a}_0)\\&-J_{\rm c}(\hat{a}_1^\dagger\hat{a}_0+\hat{b}_1^\dagger\hat{b}_0+{\rm H.c.})\\&-J_{\rm l}\sum_{j=1}^{\infty}(\hat{a}_{j+1}^\dagger\hat{a}_j+\hat{b}_{j+1}^\dagger\hat{b}_j+{\rm H.c.}),\end{aligned}\tag{1}$$

where $\hat{a}_{j\geq1}$ and $\hat{b}_{j\geq1}$ are the annihilation operators for the left or right j-th site, and $\hat{a}_0$ and $\hat{b}_0$ correspond to the locally trapped central sites. A constant term U characterizes the time-independent on-site particle interactions, while $g_a(t)=g_a\sin(\omega t)\theta(t)$ and $g_b(t)=g_b\sin(\omega t-\phi)\theta(t)$ are the periodic drives exerted to each site, with $g_{a,b}$ representing the drive strengths, ω the drive frequency, ϕ the relative phase, and $\theta(t)$ the step function.

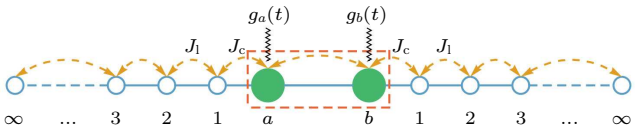


Fig. 1. A sketch of the infinite lattice. Two locally trapped sites a and b are coupled, which enables atoms to tunnel back and forth, and the pairwise interaction of atoms on these two sites has strength U. The red dashed box indicates the local trap, and the sites on each lead are labeled by $1,2,3,\ldots,\infty$.

Such an inhomogeneous lattice model with spatially localized interactions can be implemented in an experiment by the literal combinations of optical lattices and microtraps,[32] where one could routinely engineer an array of Bose–Einstein condensates in the lattices with a trap and barriers confining the central sites, and modulate the time- and space-dependent interactions through magnetic field driven Feshbach resonances.[17,18] Our work, however, is not a proposal for a particular experiment. Nevertheless, we provide a simple model whose exploration gives insight into the observations made in a more complicated study.

The formalism of such a system can be developed along the same lines as in previous works.[27,28] We introduce, in the context of mean-field approach, the expectation values of $a_{j\geq0}=\langle\hat{a}_{j\geq0}\rangle$ and $b_{j\geq0}=\langle\hat{b}_{j\geq0}\rangle$, where their squares represent the number of particles on site j. In the fireworks experiments,[17,19–22] the average dc scattering lengths were generally kept small, and in a previous work we have demonstrated that a finite U did not qualitatively change the results,[27] thus we take the limit of $U=0$ for simplicity. We begin from the equilibrium at $g=0$, which leads to the Heisenberg equations of motion for $a_{j\geq0}$ (taking units where $\hbar=1$)

$$\begin{aligned}{\rm i}\partial_t a_0 &= \langle[\hat{a}_0,\hat{H}]\rangle\\&= Va_0+g_a\sin(\omega t)|a_0|^2a_0-J_{ab}b_0-J_{\rm c}a_1,\end{aligned}\tag{2}$$

$${\rm i}\partial_t a_1 = -J_{\rm c}a_0-J_{\rm l}a_2,\tag{3}$$

$${\rm i}\partial_t a_j = -J_{\rm l}(a_{j+1}+a_{j-1}).\tag{4}$$

Analogous equations are straightforward for $b_{j\geq0}$. To largely simplify the analysis, we deal with the above equations at the perturbative level, where the drive strength g and the coupling strength $J_{\rm c}$ are both small. The substitution of the ansatz of $a_0=\alpha\,{\rm e}^{-{\rm i}\nu t}$ and $a_{j>0}=\alpha\,{\rm e}^{-{\rm i}\nu t}\,{\rm e}^{-\kappa_{\rm l}}\,{\rm e}^{-\kappa(j-1)}$ into the equations results in $\cosh\kappa=\nu/(-2J_{\rm l})$ and $\kappa_{\rm l}=-\ln[-J_{\rm c}/(\nu+J_{\rm l}\,{\rm e}^{-\kappa})]$, and we obtain two discrete modes of the system corresponding to the energies of $\nu_-=V-J_{ab}$ and $\nu_+=V+J_{ab}$, respectively.

To observe significant particle emission, there are some restrictive conditions. The infinite lattice acts as a bath, whose spectrum is a continuum corresponding to $-2J_{\rm l}<\nu<2J_{\rm l}$. The periodic drive provides the required energy for pumping particles to the excited state, such that they can escape from the trap into the continuum. We need to be in the regime where the mode $\nu_-=V-J_{ab}$ is stable while the mode $\nu_+=V+J_{ab}$ is damped, which requires $|V-J_{ab}|>2J_{\rm l}$ and $|V+J_{ab}|<2J_{\rm l}$. Specializing to the case of $V=-|V|<0$, we reach the constraints for the trapping potential as $-J_{ab}<|V|-2J_{\rm l}<J_{ab}$.

We subsequently eliminate the leads by writing $a_1(b_1)$ as a function of $a_0(b_0)$. As a result, one can focus on the time evolution of the trapped particles, and a set of nonlinear integro-differential equations for the central sites are available,

$$\begin{aligned}{\rm i}\partial_t a_0 =& Va_0+g_a\sin(\omega t)|a_0|^2a_0-J_{ab}b_0\\&+J_{\rm c}^2\int^t G_{11}(t-\tau)a_0(\tau)\,{\rm d}\tau,\end{aligned}\tag{5}$$

$$\begin{aligned}{\rm i}\partial_t b_0 =& Vb_0+g_b\sin(\omega t-\phi)|b_0|^2b_0-J_{ab}a_0\\&+J_{\rm c}^2\int^t G_{11}(t-\tau)b_0(\tau)\,{\rm d}\tau,\end{aligned}\tag{6}$$

where $G_{j1}(t)={\rm i}^{j-2}jJ_j(2J_{\rm l}t)\theta(t)/J_{\rm l}t$ is the time-domain Green's function with $J_n(z)$ being the Bessel function of the first kind.[27] To describe the nonlinear dynamics of the system, one can directly solve Eq. (2) through Eq. (4), while we obtain the following results mainly by perturbatively solving Eqs. (5) and (6), which is applicable for small parameters of the drive strength g and the coupling strength $J_{\rm c}$.

3. Results and discussion

We assume that the parametric drive is exerted at time $t = 0$. Without any loss of generality, we induce an initially slight difference of a_0 and b_0, i.e., $a_0(t = 0) = 1.01$ and $b_0(t = 0) = 1$, to seed the system at the lowest mode of $\nu_- = V - J_{ab}$, and explore the nonlinear dynamics when the drives are varied. We also take the units $J_{ab} = 1$ in most of our numerical calculations, while reintroducing the scale J_{ab} in discussions as appropriate. There is a typical threshold for the drive strength,[28] thus only those amplitudes above the threshold are taken into account. To keep simplicity, we restrict ourselves to the short-time behavior of the trapped particles, which is sufficient for the current study, and present certain situations with typical relative phases.

3.1. Relative phase $\phi = 0$

3.1.1. Same drive strength $g_a = g_b$

We first consider the general case with equal drive strength $g_a = g_b = g$ and relative phase $\phi = 0$. As shown in Fig. 2, the drive strength $g = 0.05$ is still too small to induce significant emission within this short time. When the amplitude is increased, for generic frequencies the system keeps very stable with few trapped particles ejected. Once the frequency is tuned to $\omega = 4J_{ab}$, the pulses are visible at intermediate times, and we term it as the "resonant frequency". From $g = 0.1$ we immediately recall the two-site model,[28] while intermittent emission emerges when the drive strength is further increased to $g = 0.2$ and $g = 0.3$, which was discussed in detail in Ref. [33].

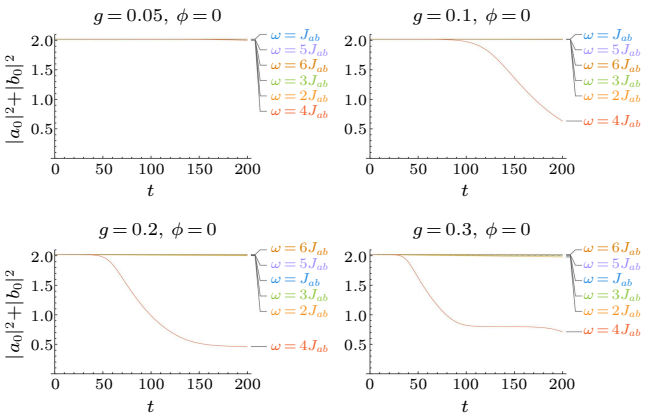


Fig. 2. Time dependence of the number of particles in the central sites $|a_0|^2 + |b_0|^2$ for equal drives $g = g_a = g_b$, under various frequencies ω. Here, the trapping potential is $V = -2$, and the coupling strengths are $J_c = 0.1$ and $J_l = 1$. Energies are in units of J_{ab} and times are in units of $\hbar/J_{ab}$.

3.1.2. Eliminating one of the drives

Next, we eliminate one of the drives by taking strength $g_b = 0$ and vary the other one g_a, which means that the manipulation is simply applied to site a, and we use $\Delta g = g_a - g_b = g_a$ to denote the imbalance of modulation amplitude. Figure 3 plainly demonstrates the distinct enhancement of particle emission that even a small imbalance of $\Delta g = 0.05$ is available for a remarkable jet, and the principal frequency becomes $\omega = 2J_{ab}$ instead of $\omega = 4J_{ab}$ under different imbalances. For $\Delta g = 0.05$ and $\Delta g = 0.1$, only the resonant frequency $\omega = 2J_{ab}$ gives rise to prominent emission, and the jet emerges much earlier than that of the cases in Fig. 2. At intermediate times $50 < t < 150$, the number of trapped particles $|a_0|^2 + |b_0|^2$ rapidly decays, leading to a large pulse until very few particles are left. For larger amplitude imbalances of $\Delta g = 0.2$ and $\Delta g = 0.3$, the frequency $\omega = 4J_{ab}$ comes into effect, while $\omega = 2J_{ab}$ results in intermittency. Note that there would be another frequency of $\omega = J_{ab}$ which can induce a slight decay within this short period of time.

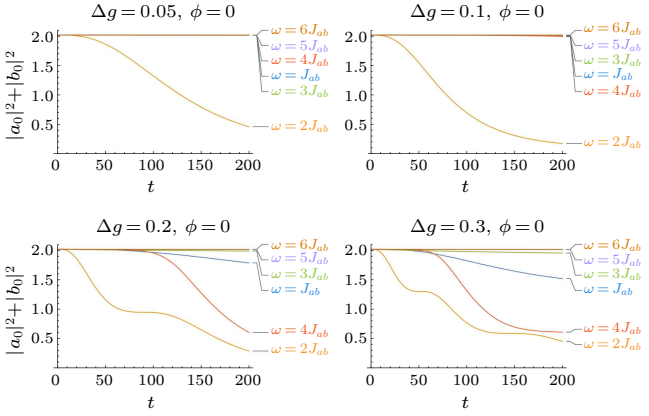


Fig. 3. Time dependence of the number of trapped particles for imbalanced drives $\Delta g = g_a$ under various frequencies ω with fixed $g_b = 0$. Here, we have taken $V = -2$, $J_c = 0.1$, and $J_l = 1$. Energies are in units of J_{ab} and times are in units of $\hbar/J_{ab}$.

Since we present, for simplicity, particular integer frequencies in the above analysis to show the main properties of the particle emission, here we take $g = \Delta g = 0.3$ as examples to sweep the frequency. Figure 4(a) shows that for equal drive strengths $g = 0.3$ and relative phase $\phi = 0$, a distinct peak appears at $\omega = 4J_{ab}$, which leads to the most significant particle emission. There is actually a narrow resonance, where the excited atoms N_e corresponding to the frequencies in between are definitely nonzero. As a comparison in Fig. 4(b), for the case with $\Delta g = 0.3$ and $\phi = 0$, the adjacent area is somewhat narrower, while a new peak with typical "bandwidth" shows up at $\omega = 2J_{ab}$, and a fairly sharp but small peak emerges at $\omega = J_{ab}$.

Under the circumstance of $g_a = g_b = g$, particles in sites a and b are simultaneously driven and they can be treated as a whole, in which the modes and energy levels are spectrally separated, as briefly depicted in Fig. 5(a). For generic drives, particles in the central sites are not directly ejected, but that promoted from the ground state of $\nu_- = V - J_{ab}$ to a higher energy level of $\nu_+ = V + J_{ab}$, namely a build-up stage at the beginning.[33] Pairs of atoms are excited at a time, and they share half of the drive energy before escaping from the trap and moving off along the leads. To this end, we need the

appropriate principal frequency that satisfies the energy gap of $\omega = 2(\nu_+ - \nu_-) = 4J_{ab}$, which corresponds to the peak in the spectrum, and there is a typical "bandwidth" that takes the level $\nu_+ = V + J_{ab}$ as the center line.

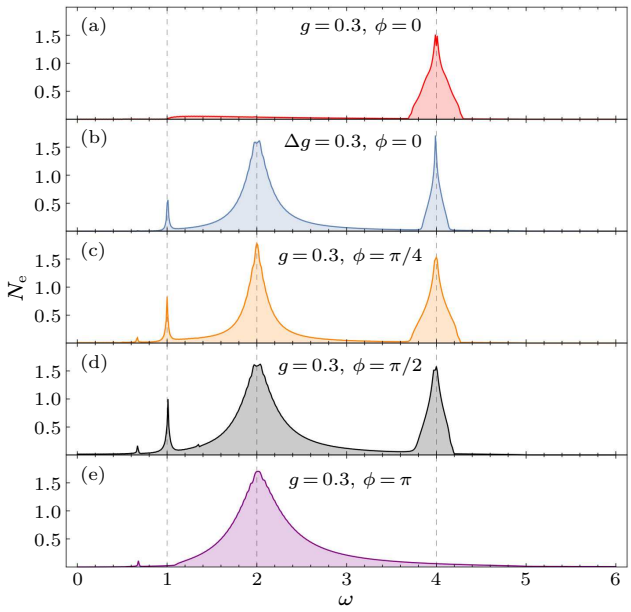


Fig. 4. Number of the excited atoms N_e versus drive frequency ω. Here, N_e is calculated from $(|a_0(t=0)|^2 + |b_0(t=0)|^2) - (|a_0(t=t_e)|^2 + |b_0(t=t_e)|^2)$ up to time $t_e = 200$, and g_b is set to be 0 with $\Delta g = g_a - g_b = 0.3$. We have taken $V = -2$, $J_c = 0.1$ and $J_l = 1$, and the frequency step is $\Delta\omega = 0.01$. Energies are in units of J_{ab} and times are in units of $\hbar/J_{ab}$.

As for the case of $\Delta g = g_a$, due to the elimination of the drive on site b, only particles in site a are subsequently stimulated when the perturbation is turned on. Site b plays the role of a "source" via the coupling, and the amplitude imbalance motivates energy shift and redistributes the energy bands, as outlined in Fig. 5(b). To be specific, under a suitable frequency around $\omega = 2J_{ab}$, half-pairs of atoms are excited from the ground state of $V - J_{ab}$ to the higher energy level of V, which takes a much shorter time in the build-up stage and emits more particles than the former case. Since the drive can provide energy in multiples, we still have another main frequency $\omega = 4J_{ab}$ that corresponds to the level of $V + J_{ab}$, but the "bandwidth" becomes narrower. The system emits a small portion of particles from the ground state to the energy level of $V - \frac{1}{2}J_{ab}$ under an approximate frequency of $\omega = J_{ab}$, by pumping single atom at a time.

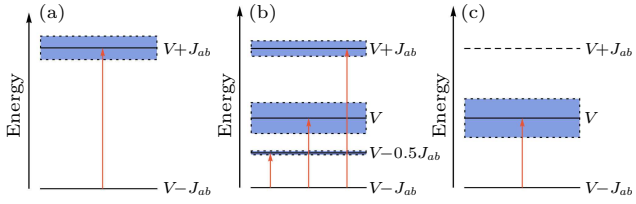


Fig. 5. Sketch of the "band structure" for cases: (a) $g_a = g_b = g$ and $\phi = 0$, (b) $\Delta g = g_a$ and $\phi = 0$, (c) $g_a = g_b = g$ and $\phi = \pi$. The blue regions indicate the dominant "bands".

From a more insightful point of view, basically the initial state with $(a_0, b_0) \simeq (1,1)$ is symmetric. When the same driving fields $g_a(t) = g_b(t)$ are applied to the central sites, the whole Hamiltonian holds a reflection symmetry that the state should maintain during the time evolution. As a consequence, the state $(1,1)$ can only evolve towards $(0,0)$, and the particle emission are typically in pairs. If one breaks the reflection symmetry, i.e., either the modulation amplitudes or the relative phases of the driving fields applied to the two central sites are imbalanced, the emission of a single particle becomes possible.

3.1.3. Fixing drive strength $g_b = \text{const.}$

We further fix one of the drive strengths $g_b \neq 0$ while varying the other one g_a. In particular, we keep $g_b = 0.3$ and present some positive $\Delta g' = g_a - g_b$ in comparison, where site b is driven persistently but the rate of particle promotion from each site varies. In this situation, the system shares similar decay properties with the former case, as shown in Fig. 6. However, when the amplitude imbalance is as small as $\Delta g' = 0.05$, there are two main frequencies $\omega = 4J_{ab}$ and $\omega = 2J_{ab}$ that give rise to significant jets. They take almost same times to result in particle jets, but frequency $\omega = 4J_{ab}$ can cause intermittency, which is somewhat different from Fig. 3. When the imbalance is $\Delta g' = 0.1$, the principal frequency gradually turns into $\omega = 2J_{ab}$ and under frequency $\omega = J_{ab}$ the system can also emit a fraction of particles. In addition, if the imbalance is further increased to $\Delta g' = 0.2$ and $\Delta g' = 0.3$, the frequency $\omega = J_{ab}$ would induce intermittency as well.

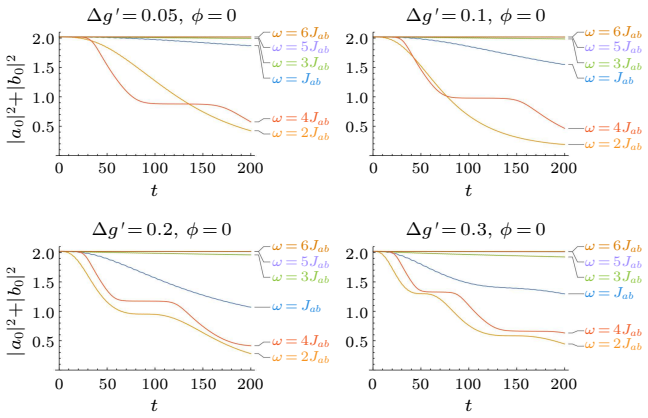


Fig. 6. Typical examples of the time evolution of the trapped particles for different $\Delta g' = g_a - g_b$ under different frequencies ω with fixed $g_b = 0.3$. Here, $V = -2$, $J_c = 0.1$, and $J_l = 1$. Energies are in units of J_{ab} and times are in units of $\hbar/J_{ab}$.

3.2. Relative phase $\phi \neq 0$

Phase difference often plays an important role in nonequilibrium quantum dynamics. In the above considerations, we neglect its influence by simply taking the relative phase as $\phi = 0$. Here, we reintroduce that the driving applied to site b holds a relative phase discrepancy when the perturbation of site a is turned on, while keeping the drive strengths as

$g_a = g_b = g = 0.3$. We scan the frequency and calculate the number of excited atoms on each site, and present the comparisons among some typical relative phases of $\phi = \pi/4$, $\pi/2$ and π, as shown in Figs. 4(c)–4(e).

Compared to Fig. 4(a) one can plainly see that the nonzero relative phase $\phi \neq 0$ makes the "bandwidth" at frequency $\omega = 4J_{ab}$ become thinner, while it opens another band at frequency $\omega = 2J_{ab}$, which turns to be wider as the phase difference increases from $\pi/4$ to $\pi/2$. When the relative phase is $\phi = \pi$, the peak at frequency $\omega = 4J_{ab}$ vanishes, and there is only a distinctly wide band around frequency $\omega = 2J_{ab}$, as depicted in Fig. 5(c). It is interesting to note that these two cases with relative phases $\phi = \pi/4$ and $\phi = \pi/2$ share similar properties to that of the situation with amplitude imbalance $\Delta g = 0.3$ and relative phase $\phi = 0$, which means that in experiments one can probably, based upon demand, manage to induce analogous effects by generating either amplitude imbalance or phase difference.

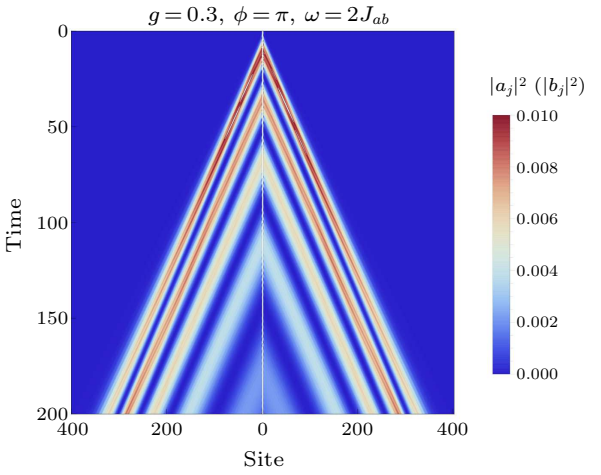


Fig. 7. Time evolution of the particles on jth site in the left or right lead under a typical drive frequency $\omega = 2J_{ab}$, when the drive strength is $g = g_a = g_b = 0.3$ and the relative phase is $\phi = \pi$. Here, $V = -2$, $J_c = 0.1$ and $J_l = 1$. Energies are in units of J_{ab} and times are in units of $\hbar/J_{ab}$.

To be more explicit, for relative phase $\phi = 0$ sites a and b are driven simultaneously by same drives, such that one returns to the general case of $g_a = g_b$. As for nonzero phases, e.g., $\phi = \pi/4$, there has been a difference between the two separate drives. They deviate from $g_a(t = 0) = 0$ and $g_b(t = 0) = 1/\sqrt{2}$, and then $\Delta g(t)_{\phi=\pi/4} = \sin(\omega t) - \sin(\omega t - \pi/4)$, which is in fact the situation of the former case with $\Delta g = g_a - g_b$ in Fig. 3. Therefore, under these two cases the system shares similar characteristics, and the amplitude imbalance Δg grows with the increase of $\phi \leq \pi/2$. Once the relative phase is tuned to $\phi = \pi$, the resulting amplitude imbalance $\Delta g = g_a - g_b = 2\sin(\omega t)$ is twice of the generic case, leading to the shift of the main frequency from $\omega = 4J_{ab}$ to $\omega = 2J_{ab}$, as well as the broadening of the bandwidth. As a specifically visible example, we present in Fig. 7 the intermittent antipodal jets under drive frequency $\omega = 2J_{ab}$, by plotting the number of particles on each site in the left or right lead.

4. Conclusions

We have introduced a one-dimensional infinite lattice, in which the trap confines two central sites, and studied the influences of drive imbalance on the collective particle emission from a Bose–Einstein condensate. We follow the formalism developed in previous works to parametrically modulate the particle interactions, while separately varying the periodic drives in modulation amplitudes and relative phases.

Within perturbative analysis and numerical calculations, we find that the modulation amplitude imbalance may result in the enhancement of particle emission and redistribute the band structures, where even a small drive gives rise to significant particle jets, energy shift and band broadening. Moreover, relative phases can lead to similar band gaps, where the effect induced by nonzero phase difference is basically analogous to that of the modulation amplitude imbalance. One can thus, for certain purpose, employ either method in precise quantum manipulations in experiments.

There have been a number of recent explorations with respect to two-frequency phase modulations[21,29–31] both in one and two dimensions. The geometry of the system and the boundary condition typically play a role in the excitations. If one explicitly follows the methodology, the dynamics of the lattice systems would be particularly interesting. Such influence of parametric drives with varied frequencies on distinct configurations is worth investigating, and we leave it for future research.

Acknowledgments

Project supported by the China Scholarship Council (Grant No. 201906130092), the Natural Science Research Start-up Foundation of Recruiting Talents of Nanjing University of Posts and Telecommunications (Grant No. NY223065), and the Natural Science Foundation of Sichuan Province (Grant No. 2023NSFSC1330).

References

[1] Chevy F and Mora C 2010 *Rep. Prog. Phys.* **73** 112401
[2] Nandkishore R and Huse D A 2015 *Annu. Rev. Condens. Matter Phys.* **6** 15
[3] Zhang Z, Chen L, Yao K X and Chin C 2021 *Nature* **592** 708
[4] Langen T, Geiger R and Schmiedmayer J 2015 *Annu. Rev. Condens. Matter Phys.* **6** 201
[5] Moon G, Heo M S, Kim Y, Noh H R and Jhe W 2017 *Phys. Rep.* **698** 1
[6] Bloch I, Dalibard J and Nascimbene S 2012 *Nat. Phys.* **8** 267
[7] Lewenstein M, Sanpera A and Ahufinger V 2012 *Ultracold atoms in optical lattices: Simulating quantum many-body systems* (Oxford: Oxford University Press)
[8] Georgescu I M, Ashhab S and Nori F 2014 *Rev. Mod. Phys.* **86** 153
[9] Eckardt A 2017 *Rev. Mod. Phys.* **89** 011004

[10] Jotzu G, Messer M, Desbuquois R, Lebrat M, Uehlinger T, Greif D and Esslinger T 2014 *Nature* **515** 237

[11] Aidelsburger M, Lohse M, Schweizer C, Atala M, Barreiro J T, Nascimbène S, Cooper N R, Bloch I and Goldman N 2015 *Nat. Phys.* **11** 162

[12] Dalibard J, Gerbier F, Juzeliūnas G and Öhberg P 2011 *Rev. Mod. Phys.* **83** 1523

[13] Krämer M, Tozzo C and Dalfovo F 2005 *Phys. Rev. A* **71** 061602

[14] Cabrera-Gutiérrez C, Michon E, Arnal M, Chatelain G, Brunaud V, Kawalec T, Billy J and Guéry-Odelin D 2019 *Eur. Phys. J. D* **73** 170

[15] Arnal M, Chatelain G, Cabrera-Gutiérrez C, Fortun A, Michon E, Billy J, Schlagheck P and Guéry-Odelin D 2020 *Phys. Rev. A* **101** 013619

[16] Wintersperger K, Bukov M, Näger J, Lellouch S, Demler E, Schneider U, Bloch I, Goldman N and Aidelsburger M 2020 *Phys. Rev. X* **10** 011030

[17] Clark L W, Gaj A, Feng L and Chin C 2017 *Nature* **551** 356

[18] Chin C, Grimm R, Julienne P and Tiesinga E 2010 *Rev. Mod. Phys.* **82** 1225

[19] Fu H, Feng L, Anderson B M, Clark L W, Hu J, Andrade J W, Chin C and Levin K 2018 *Phys. Rev. Lett.* **121** 243001

[20] Fu H, Zhang Z, Yao K X, Feng L, Yoo J, Clark L W, Levin K and Chin C 2020 *Phys. Rev. Lett.* **125** 183003

[21] Zhang Z, Yao K X, Feng L, Hu J and Chin C 2020 *Nat. Phys.* **16** 652

[22] Mežnaršič T, Žitko R, Arh T, Gosar K, Zupanič E and Jeglič P 2020 *Phys. Rev. A* **101** 031601

[23] Chen T and Yan B 2018 *Phys. Rev. A* **98** 063615

[24] Wu Z G and Zhai H 2019 *Phys. Rev. A* **99** 063624

[25] Chih L Y and Holland M 2020 *New J. Phys.* **22** 033010

[26] Lellouch S and Goldman N 2018 *Quantum Sci. Technol.* **3** 024011

[27] Lai L Q, Yu Y B and Mueller E J 2021 *Phys. Rev. A* **104** 033308

[28] Lai L Q, Yu Y B and Mueller E J 2022 *Phys. Rev. A* **106** 033302

[29] Sandholzer K, Walter A S, Minguzzi J, Zhu Z, Viebahn K and Esslinger T 2022 *Phys. Rev. Res.* **4** 013056

[30] Wang Y, Walter A S, Jotzu G and Viebahn K 2023 *Phys. Rev. A* **107** 043309

[31] Minguzzi J, Zhu Z, Sandholzer K, Walter A S, Viebahn K and Esslinger T 2022 *Phys. Rev. Lett.* **129** 053201

[32] Kaufman A M and Ni K K 2021 *Nat. Phys.* **17** 1324

[33] Lai L Q, Li Z, Liu Q H and Yu Y B 2022 arXiv:2211.03386 [cond-mat.quant-gas]